Instability and Finite-Amplitude Self Organization of Large-Scale Coastline Shapes

A. Brad Murray[1]

Andrew D. Ashton[2]

1. Duke University, Nicholas School of the Environment; Center for Nonlinear and Complex Systems, Box 90230, Durham, NC, USA. abmurray@duke.edu

2. Woods Hole Oceanographic Institution, Geology and Geophysics Department, 360 Woods Hole Rd. Woods Hole, USA. aashton@whoi.edu

Abstract

Recent research addresses the formation of patterns on sandy coastlines on alongshore scales that are large compared to the cross-shore extent of active sediment transport. A simple morphodynamic instability arises from the feedback between wave-driven alongshore sediment flux and coastline shape. Coastline segments with different orientations experience different alongshore sediment fluxes, so that curvatures in coastline shape drive gradients in sediment flux, which can augment the shoreline curvatures. In a simple numerical model, this instability, and subsequent finite-amplitude interactions between pattern elements, lead to a wide range of different rhythmic shapes and behaviours—ranging from symmetric cuspate capes and bays to alongshore migrating 'flying spits'—depending on the characteristics of the input wave forcing. The scale of the pattern coarsens in some cases because of the merger of migrating coastline features, and in other cases because of non-local screening interactions between coastline protrusions, which affect the waves reaching other parts of the coastline. Features growing on opposite sides of an enclosed water body mutually affect the waves reaching each other in ways that lead to the segmentation of elongated water bodies. Initial tests of model predictions and comparison with observations suggest that modes of pattern formation in the model are relevant in nature.

Keywords: Coastlines, pattern formation, high-angle waves, emergent structures, non-local interactions

1 Introduction

In Earth-surface environments, pattern formation often occurs through morphodynamic processes in which fluid flow, sediment transport, and bed morphology co-evolve through mutual interactions. Patterns of water flow on river and sea beds, and wind blowing across sandy surfaces, create patterns of sediment flux that alter the shape of the surface—which in turn alters the patterns of flow (e.g. {Andreotti, 2002 #1856;Charru, 2013 #1857;Coco, 2007 #1855;Kocurek, 2010 #1858}). These feedbacks often lead to instabilities in which an initially smooth morphologic configuration is unstable to infinitesimal perturbations, e.g. to the shape of the sediment bed. As bumps on a bed grow to finite amplitude, they begin to interact with each other in diverse ways that lead to an array of captivating patterns including familiar ripples generated by the wind, waves, or currents; desert sand dunes; and arrays of bars and channels in rivers and shallow seabeds.

Here we review a particular set of morphodynamic pattern formation processes that can shape sandy coastlines. These processes are relatively recently understood, and the resulting patterns differ from many familiar Earth-surface patterns in two ways. First, instead of consisting of topographic bumps—vertical deviations relative to a horizontal surface—the coastline patterns we will focus on are primarily horizontal bumps, i.e. shoreline shapes drawn in a horizontal plane. Because of this, gravitational influences on sediment fluxes do not play the same role in shaping the coastline patterns that they do for topographic bump patterns that fundamentally involve elevation gradients and therefore downslope sediment fluxes that tend to inhibit the growth of pattern elements. Although other processes tend to smooth coastline shapes (e.g. gradients in alongshore sediment flux, as we discuss below), the lack of a horizontal equivalent to gravity can lead to a wider diversity of shapes and finite-amplitude interactions between coastline-pattern elements than is possible for topographic patterns such as bedforms. (The plan-view pattern of one well-studied morphodynamic system, meandering rivers, exhibit a similar lack of direct gravitational constraint, with the amplitude and complexity of meander loops limited mainly through their interactions with each other.)

Second, the coastline patterns we will focus on can occur on scales much larger than most other patterns with a morphodynamic origin. In coastal environments, myriad interesting patterns and dynamics occur on scales commensurate with those of waves , or the width of the zone of breaking waves (the 'surf zone') {Coco, 2007 #1855}. However, in this limited review we will discuss only a particular set of processes that involve alongshore scales much larger than the width of surf zone, and even larger than the width of the nearshore swath of seabed that commonly experiences wave-influenced sediment transport (the 'shoreface'). While these scales can be relatively small in small water bodies that limit the size of waves, for shorelines subject to large ocean waves, the minimum alongshore scale at which the dynamics we will summarize become important is several kilometers {Falqués, 2005 #1433;Falqués, 2011 #1854; van den Berg, 2011 #1853}, and the resultant patterns can attain scales on the order of 100 kilometers.

2 Background: Alongshore Sediment Flux and Wave Angles

The coastline shapes we focus on arise from wave-driven alongshore sediment flux. Alongshore changes in coastline orientation tend to induce alongshore variations in local wave conditions, and therefore gradients in alongshore sediment flux. These flux gradients tend to cause the shoreline to build seaward in some places (where sediment flux converges), and to erode landward in others (where sediment flux diverges), as expressed by the continuity equation:

$$\frac{\partial \eta}{\partial t} = \frac{1}{D}\frac{\partial Q_s}{\partial x}, \quad (1)$$

where η is the cross shore position, x is the (local) alongshore coordinate, t is time, Q_s is total alongshore sediment flux (total volume per time unit that crosses a cross-shore section), and D is the depth to which sediment is eroded from or spread across the seabed. The changes in shoreline position, in turn, change the plan-view shape of the coastline, and therefore the patterns of sediment flux, completing the morphodynamic loop. (Although other processes also cause shoreline change, on long time scales and large spatial scales, gradients in alongshore transport tend to dominate shoreline change, as outlined in the Discussion section.) To better understand this morphodynamic loop, we need to understand how alongshore sediment flux depends on local shoreline orientation.

A Breaking Wave View

Wave-driven alongshore sediment flux occurs primarily in the surf zone, where a usually subtle alongshore current advects sand that is suspended by wave-breaking turbulence. Wave momentum drives the alongshore current. The organized motion of water particles associated with waves constitutes a momentum flux across a plane oriented perpendicular to the wave propagation direction. Just as random molecular motions lead to macroscopic pressure, when averaged over time scales longer that a wave period, the organized momentum flux from wave motions can be treated as stress {Longuet-Higgins, 1970 #1275}. (In addition to the directional component from organized water motions, dynamic pressure effects lead an isotropic component to this stress, beyond the hydrostatic pressure in the absence of waves.) Gradients in this 'radiation stress' represent a force, just as gradients in pressure do.

In the surf zone, where waves break and dissipate, the resultant radiation stress gradient pushes water in the direction of wave propagation. The cross-shore component of this force tends to create a water surface slope in the cross-shore direction, which leads to secondary, residual cross-shore currents {Fredsoe, 1992 #1248}. The alongshore component of this force drives an alongshore current that can only be balanced by frictional forces. The steady-state velocity of this alongshore current depends on the rate that waves bring alongshore momentum into the surf zone, and is therefore a function of the height of the waves as they break and of the angle the breaking waves make with the shoreline (the 'breaking angle') {Fredsoe, 1992 #1248} (Figure 1a).

Holding the breaking wave height constant, as the breaking angle increases, the alongshore component of the wave forcing—and therefore the magnitude of the alongshore current and associated sediment flux—increases. If a coastline is curved, the breaking angles will tend to vary moving alongshore as coastline orientation varies. This will result in a gradient in the alongshore sediment flux.

However, for a given offshore wave condition, changing breaking angles from one location to another tend to be associated with changes in breaking wave heights (Figure 2). (Greater wave angles in shallow water tend to be associated with more nearshore refraction, which stretches wave crest and reduces wave height.) This dependence between breaking wave angles and heights complicates an analysis of how alongshore sediment flux depends on coastline orientation that focuses on breaking-wave characteristics. Ashton et al. {, 2001 #1788} present a more parsimonious analysis based instead on the characteristics of offshore waves—before they are affected by nearshore bathymetry.

An Offshore Wave View

A consideration of some basic physics is sufficient to understand the qualitative aspects of the relationship between offshore wave angle and alongshore sediment transport. Holding offshore wave height constant and assuming shore-parallel bathymetric contours, we consider two limits. First, if the offshore wave crests parallel the shoreline (an angle of 0° between wave crests and the shoreline), then the breaking wave angle will also be 0°; the alongshore component of the wave momentum flux entering the surf zone, and therefore the alongshore sediment flux, will be zero. Increasing offshore wave angle from this limit will tend to increase alongshore sediment flux (a positive derivative for left-hand portion of the sediment flux-wave angle curve, Figure 1b).

In the other limit, if the offshore wave angle is 90°, then wave energy and momentum is propagating in the alongshore direction, and the flux of energy and momentum toward shore is zero. Decreasing the offshore angle from this limit will tend to increase the rate of energy and momentum transmission into the surf zone, and therefore increase the alongshore sediment flux (a negative derivative for the right-hand portion of the sediment flux-wave angle curve, Figure 1b). Somewhere in between the two limits, the competing limitations on alongshore sediment flux will have an equal effect, and the function relating alongshore sediment flux to offshore wave angle will exhibit a maximum.

To quantify this relationship, we assume shore-parallel nearshore contours (an important approximation {Falqués, 2005 #1433;Falqués, 2011 #1854;van den Berg, 2011 #1853; van den Berg, 2012 #1862} that improves as alongshore spatial scales exceed width of the shoreface—see the Discussion section), and neglect wave dissipation during nearshore wave transformation. With these approximations, a semi-empirical relationship for alongshore sediment flux as a function of breaking-wave quantities:

$$Q_s = K_1 H_b^{5/2} cos(\phi_b - \theta) sin(\phi_b - \theta) \quad (2)$$

can be transformed into a relationship involving offshore wave characteristics {Ashton, 2001 #1788;Ashton, 2006 #1466}:

$$Q_s = K_2 H_0^{12/5} T^{1/5} cos(\phi_0 - \theta)^{6/5} sin(\phi_0 - \theta) \quad (3)$$

where H is the wave height (m), T is the wave period (s), ϕ is the wave crest angle, θ is the shoreline orientation, K_1 is an empirical coefficient here set equal to 0.4 $m^{1/2}s^{-1}$ (K_1 can span an order of magnitude around this value), K_2 accordingly equals ~ 0.34 $m^{3/5}s^{-6/5}$, and the subscripts $_b$ and $_0$ denote breaking and offshore-water wave quantities, respectively (Figure 1a). Figure 1b shows the angle dependence of (3),

normalized for a given wave height. Although other formulations for alongshore sediment transport, when transformed into offshore quantities, predict slightly different curves, all produce a maximum in sediment flux for offshore wave angles around 45° {Ashton, 2006 #1469}.

3 An Instability in Coastline Shape

Figure 1b leads to basic insights regarding coastline dynamics. Picture a nearly straight coastline with a subtle (infinitesimal amplitude) plan-view perturbation. If the offshore wave characteristics are constant in the alongshore direction, then alongshore variations in local coastline orientation alone produce gradients in alongshore sediment flux.

If the offshore wave angle, relative to the overall coastline orientation, is lower than the angle that will maximize the alongshore sediment flux ('low-angle' waves), then convex-seaward coastline curvature will produce a divergence of sediment flux. In this case, moving alongshore in the direction of sediment transport, the offshore angle relative to the local coastline orientation comes progressively closer to the flux-maximizing angle between the inflection points on the coastline bump in Figure 2. (In Figure 1b, this corresponds to moving to the right along the left hand portion of the curve.) The divergence of sediment flux will cause the 'crest' of the bump to erode landward. Conversely, areas with concave-seaward curvature, such as those flanking the bump, will experience converging sediment flux, and therefore seaward shoreline accretion. Thus, under the influence of low-angle waves, coastline bumps tend to be progressively smoothed.

On the other hand, if the offshore waves have an angle greater than the one the maximizes the sediment flux ('high-angle' waves), then areas of convex-seaward curvature feature converging sediment flux, and therefore seaward accretion, while convex areas experience a divergence of sediment flux and therefore erosion; high-angle waves tend to cause coastline bumps to become exaggerated (Figure 2). In other words, under the influence of high-angle waves, a straight coastline is an unstable configuration.

It is useful to note that breaking wave angles are expected to be always much smaller than 45°, even when offshore waves are approaching from 'high' angles, and that in the case of high-angle waves, breaking-wave angles tend to be rather similar along the coast. Variation in wave height, resulting from different amounts of energy spreading by wave refraction, drive gradients in the alongshore sediment transport (Figure 2).

By combining equations (1) and (3), and making small-angle approximations (specifically that deviations in local shoreline orientations relative to the overall coastline orientation are small), we can derive a diffusion equation for coastline shape (in which coastline position, rather than sediment, diffuses in the alongshore direction):

$$\frac{\partial \eta}{\partial t} = K_2 H_0^{12/5} T^{1/5} \psi \frac{\partial^2 \eta}{\partial x^2} \quad (4)$$

where the angle dependence of shoreline shape diffusivity is given by:

174 $$\psi = cos(\phi_0 - \theta)^{1/5}\left\{cos^2(\phi_0 - \theta) - \tfrac{6}{5}sin^2(\phi_0 - \theta)\right\}. \quad (5)$$

175 This formulation shows that when offshore wave angles are greater than approximately 45° (42° in this
176 formulation, although using a different alongshore-sediment-flux relationship would shift the exact
177 value of the critical angle slightly), the effective diffusivity becomes negative, reflecting the instability in
178 coastline shape. When offshore waves approach at low angles, diffusivity is positive, reflecting the
179 shoreline smoothing influence of such waves (Figure 1c).

180 Equation (4) involves significant limitations, however. Because waves approach from different directions
181 on different days, an instantaneous diffusivity, related to a single wave-approach direction, does not
182 characterize long-term evolution well. Rather, the diffusivities related to waves coming from a range of
183 different directions should be weighted by the relative influences on alongshore sediment transport
184 from waves coming from those respective directions {Ashton, 2006 #1469;Ashton, 2003 #1420;Falqués,
185 2006 #1892}. The resulting effective diffusivity can characterize the conditions affecting a specific
186 coastline. Alternatively, simplified 'wave climates' can by synthesized to explore the results of different
187 mixes of wave influences from different directions, as we present in the next sections.

188 Another reason for caution in interpreting equations (4) and (5) stems from the assumption in the
189 derivation of equation (3) and therefore equation (5) that waves refract and shoal over shore-parallel
190 contours. This assumption amounts to neglecting curvatures in shoreface contours. Accounting for the
191 curvature of those contours in a numerical wave-transformation model alters the distribution of
192 breaking wave height and angles along an undulating shoreline, relative to the results of neglecting that
193 curvature {Falqués, 2005 #1433}. Although the approximation of shore-parallel contours improves as the
194 alongshore scale of coastline undulations becomes large relative to the cross-shore scale of the
195 shoreface (please see the Discussion section), when alongshore scales become small, curvatures in
196 shoreface contours become more important, with the result that undulations below a certain
197 alongshore length scale (which depends on wave and shoreface characteristics) are stable, even when
198 equations (4) and (5) would predict instability (for high-angle offshore waves) {Falqués, 2005
199 #1433;Falqués, 2011 #1854;van den Berg, 2012 #1862}. This important caveat means that equations (4)
200 and (5) should not be taken literally in the limit of small alongshore wavelength, which alleviates the
201 potential concern for unsavory behavior (infinite growth rates) in the limit of small scales associated
202 with a negative diffusivity. Models including contour curvature effects predict that the growth rates are
203 maximum for a finite alongshore length scale (on the order of 1 – 10 km for open-ocean coastlines)
204 {Falqués, 2005 #1433;Falqués, 2011 #1854;van den Berg, 2011 #1853}.

205 In addition, in the case where the long-term effective diffusivity is negative (instability), a diffusion
206 equation only alludes to the initial growth of coastline perturbations. We present equations (4) and (5)
207 only to help illustrate the instability (valid in the limit of large alongshore scales). As bumps grow to
208 finite amplitude, exhibiting a greater range of coastline orientations, the approximation that variations
209 in local coastline orientation relative to the overall coastline orientation are small become
210 inappropriate. Finite-amplitude shape evolution will, generally, deviate from simple anti-diffusion.
211 Perhaps more interestingly, different finite amplitude features growing along the same coastline could

interact with each other in ways that guide the pattern evolution beyond the initial-instability stages. To explore these finite-amplitude effects, we turn next to a simple numerical model and some basic results.

4 Open Coastline Patterns

The numerical model introduced by Ashton et al. {, 2001 #1788}, and described in detail by Ashton and Murray {, 2006 #1466}, discretizes equations (1) and (2) across a two-dimensional plan-view domain (Figure 3). A new offshore wave direction (spatially uniform along the domain) is chosen each model day from a probability distribution that can be based on observed wave climates {Ashton, 2006 #1469}, or, for more exploratory investigations, can be controlled by two simple parameters: U, the proportion of wave influences coming from high angles, and A, wave-climate asymmetry, or the proportion of wave influences coming from the left, when looking offshore. Although wave heights tend to be correlated with offshore wave-approach directions on natural coastlines (as strong storms tend to generate large waves from certain directions), in the model representation of wave climates the offshore wave height is held constant, and the relative influences on alongshore transport from different directions is accounted for by adjusting the proportion of waves coming from each wave-angle bin.

In each model grid cell, nearshore wave transformations—the result of changes in wave propagation velocity as water depth decreases—are calculated assuming that nearshore seabed contours parallel the local shoreline orientation. Wave height and angle are iteratively adjusted until depth-limited breaking occurs. Then, the breaking wave height and angle (relative to the local shoreline) are input into equation (2).

Although the representations of various processes and factors have been subsequently incorporated in the model (including the effects of varying shoreline geology/lithology and fluvial sediment sources) {Valvo, 2006 #1442;Ashton, 2011 #1815;Ashton, 2012 #1819}, in the results we present here, only two additional influences augment shoreline changes driven by alongshore sediment flux gradients. This basic model incorporates wave shadowing—the tendency for a coastline protrusion to protect some coastline segments from a given wave-approach direction (Figure 3). In the model, a simple geometric rule determines which shoreline cells are in shadow during a model iteration, and in those shadowed cells, sediment flux is zero during that iteration. In addition, in some model runs, a representation of the effects of storm-driven barrier 'overwash' enforces a minimum width for elongated coastline features.

A variety of shoreline shapes emerge from the simple model interactions, depending on the characteristics of the wave climate, defined by U and A (Figure 4) {Ashton, 2006 #1466}.

Nearly Symmetric Wave Climates

For symmetric, or nearly symmetric wave climates, features termed 'cuspate capes' rapidly attain a steady-state shape and aspect ratio (cross-shore amplitude/alongshore wavelength), with aspect ratio increasing as U is increased (Figure 4). However, the scale of the pattern continuously increases (coarsens). With wave-climate symmetry, shoreline features do not migrate alongshore, so the coarsening is not a result of mergers between features with different propagation velocities, as occurs in many other morphodynamic pattern forming systems {Fourrière, 2010 #1859;Murray, 2004

#1551;Werner, 1993 #1860}. Observation of model results presents clues to the mechanism behind the coarsening: a secondary instability involving wave shadowing (Figure 5).

When neighboring capes exhibit nearly, but not quite, the same cross-shore extent, the feature that protrudes farther seaward will shadow the slightly smaller neighbor from some of the highest-angle waves (Figure 5). This changes the local wave climate at the seaward 'nose' of the slightly smaller neighbor, making the effective diffusivity at the crest less negative. Thus, the slightly larger neighbor will tend to grow, relative to the smaller one. Then, as a result, the shadowing effect becomes more pronounced. This 'screening' mechanism and feedback eventually makes the effective diffusivity at the crest of the smaller neighbor become positive, and the smaller feature then rapidly disappears, abruptly causing a punctuated increase in the average wavelength, and an associated shifting of the positions of the remaining features. Interestingly, the rate of coarsening with symmetric (or nearly symmetric) wave climates follows a diffusive time-space scaling, despite the non-linear, non-local interactions involved {Ashton, 2006 #1466}.

Examining this coarsening mechanism highlights a fundamental difference between the dynamics of infinitesimal-amplitude bumps on a nearly straight coastline and finite-amplitude features on a more complex coastline. On a nearly straight coastline, local shoreline change can be related to local coastline curvature, with a spatially uniform effective diffusivity. However, changes on a coastline with a finite-amplitude pattern involve both local shoreline curvatures and variations in local effective diffusivity. The way the cuspate pattern organizes itself in the model, for example, only the tips of the capes experience an effective diffusivity that is negative; the rest of the coastline is subject to the smoothing influence of positive local effective diffusivities (Figure 5b). Variations in local effective diffusivities, relative to the effective diffusivity of the regional (model input) wave climate, arise both from shadowing effects (Figure 5c), and from changes in local shoreline orientation. Changes in local shoreline orientation, relative to the regional coastline orientation (model initial condition), alter both the waves that approach that shoreline, and the angle those waves have relative to that shoreline orientation.

Because the local effective diffusivities can vary drastically over a small portion of the pattern—such as in the vicinity of the cape tip—analyzing local coastline change with a diffusion-equation framework would require including a term representing the spatial gradient in effective diffusivity.

Asymmetric Wave Climates

When wave climates are moderately asymmetric and moderately dominated by high-angle waves, alongshore-migrating features that maintain an approximately constant shape result. These shapes can be subtle ('sandwaves') or exhibit larger aspect ratios as U and/or A increase (Figure 4). Interactions between migrating features, including overtaking and mergers, again lead to pattern coarsening with time.

If U and/or A are sufficiently large, migrating features eventually sprout 'flying spits', which change the style of migration and long-range interaction. In contrast to the alongshore propagation of coastline shape, which arises from the pattern of gradients in a spatially continuous alongshore sediment flux, the rate at which the end of a spit propagates depends on the magnitude of alongshore sediment flux—

since all of the sediment is trapped at the end of a growing spit. Coastline change shifts from the flux-gradient mode to the flux-magnitude mode when the local shoreline orientation at the 'downdrift' (analogous to 'downstream') inflection point of a coastline bump deviates from the regional orientation enough (in concert with shadowing effects from other features) to produce a net alongshore flux of 0 locally. As the resulting spits elongate, they take on an orientation that maximizes the net alongshore sediment flux {Ashton, 2006 #1469;Ashton, 2007 #1644} maximizing the alongshore propagation of the spit tip.

In addition, an extending spit radically changes the local wave climates felt in adjacent parts of the coastline in the downdrift direction. By screening out the high-angle waves coming from the dominant direction, the spit creates a zone subject to positive diffusivity and coastline smoothing (Figure 4). Thus, a growing spit tends to eliminate growing features downdrift of it. On the other hand, deep in the shadows of a flying spit, the local wave climate can be dominated by the high-angle waves coming from the non-dominant direction, causing coastline features to grow and migrate in the overall 'updrift' direction—sometimes smaller flying spits—that then eventually merge onto the underside of the larger flying spit (Figure 4).

5 Enclosed Water Bodies

Considering these pattern formation dynamics in the context of enclosed lakes or bays brings up new modes of interaction between finite-amplitude growing features {Ashton, 2009 #1710}. Unlike on an open coastline, where we can consider the offshore waves to be approximately uniform in the alongshore direction, in an enclosed water body, the size of the offshore waves (before they interact with shore-parallel bathymetry) depend on the distance to the opposite shore in the direction the wind is coming from. This wind 'fetch', and therefore the size of the waves, in general varies from one location to another along the shore.

The fetch dependence means that even if the distribution of wind directions is isotropic, anisotropy in the shape of the water body leads to preferred directions for wave generation. In an elongated water body, winds blowing along the long axis (or close to it) will generate larger waves than winds blowing across the short axis. Therefore, the shorelines along the water body will tend to be dominated by high-angle waves (except for the shorelines near the ends of the water body, to which waves moving along the long axis are low-angle waves). If the wind climate is isotropic, then shorelines near the middle of the elongated water body will tend to experience approximately symmetric wave climates, while local wave climates farther from the middle will feel increasingly asymmetric climates. If the shorelines of the water body consist of mobile sediment (sand or gravel), then cuspate capes will tend to form on either side near the middle, while flying spits will arise closer to the ends, migrating toward the ends of the water body {Ashton, 2009 #1710}.

Thus, an isotropic water body, with a scale smaller than the characteristic scale of the storms that generate winds, will create its own high-angle waves and associated morphodynamics, without relying on a fortuitous dominance of waves approaching from certain directions as on open-ocean coastlines.

In addition, in an enclosed water body, growing shoreline features not only interact with their neighbors in the alongshore direction, but also with features on the opposite shoreline. A growing shoreline protrusion across the water body tends to reduce the fetch, and therefore the waves, felt on the shoreline of interest. Directly across the water body from a large shoreline feature, therefore, local wave climates tend to be even more dominated by high angle waves (since the wave coming nearly straight across the water body will be smaller). This increase in high-angle influences will tend to increase the aspect ratio of features growing on the coastline of interest (Figure 4). Of course, the features on the coastline of interest are also affecting local wave climates across the water body—tending to make the features there protrude farther, which enhances the changes in local wave climates on the shoreline of interest (Figure 6).

Growing features on the opposite shoreline—unless they are directly across the water body— also affect the asymmetry of wave climates on the shoreline of interest, tending to make the asymmetry locally point toward a growing feature across the water body (Figure 6).

The mutual interactions across the water body—both the tendency for opposing features to increase each other's aspect ratios, and the tendency to affect each other's asymmetry—lead to an attraction between features on opposite shorelines. If the aspect ratio of the initial water body is sufficiently high in the model, this attraction inevitably leads to the merger of opposite-shoreline features, and the segmentation of the elongated water body into smaller, more equant lakes or ponds. These individual segments will be round if the wind distribution of isotropic. Or, for an anisotropic wind climate, they will be nearly round, and exhibit a slow migration, as sediment is swept continuously from one side to the other. The water body moves in a direction parallel to the shoreline orientation that produces the greatest net flux for the given wind climate, but in the effective upwind direction.

6 Discussion

These model explorations reveal intriguing instabilities, emergent finite-amplitude shapes, and modes of self-organization of rhythmic patterns that apply at least in the context of the model—and possibly in nature as well. However, the modeling work reviewed here involves significant simplifications when compared to nature. The assumption that wave transformations occur over a seabed that features shore-parallel depth contours facilitates a clear analysis of the coastline instability in terms of offshore wave characteristics. However, shore parallel contours are at best an approximation of real coastlines—an approximation that becomes most realistic in the limit of large spatial and temporal scales. We consider this modeling work to be most relevant to changes on alongshore scales larger than the cross-shore width of the shoreface (typically kilometers on an open ocean coastline), and on timescale longer than the characteristic time for the cross-shore profile of the shoreface to adjust (years to decades {Stive, 1995 #1501}).

On these large spatial scales, shoreline contours do approximately parallel the coastline {Ells, 2012 #1863}. If we are interested in the evolution of coastline features on this large scale, we can probably safely neglect smaller scale features superimposed on the shoreface. (In doing this, we purposefully neglect other interesting wave-related shoreline changes {List, 2007 #1565}, in an effort to maximize the

clarity of insights regarding larger-scale interactions.) We consider the offshore extent of the shoreface to be the best interpretation of what is meant by 'offshore' waves in the context of this modeling work; from that point landward, wave shoaling and transformation is affected by approximately shore-parallel bathymetry. (Note that this interpretation does not correspond to fully deep-water waves in the technical sense {Mei, 1989 #1861}, since relatively long-period waves will already have been refracted over continental shelf contours that do not reflect the coastline shape directly. In earlier papers, the term 'deep-water' wave was misleadingly used instead of 'offshore', when referring to the seaward extent of shore-parallel contours).

In this modeling work, as a shoreline perturbation grows (or is smoothed out), it is implicitly assumed that the seabed contours exhibits the same shape change, down to the depth of the shoreface, and that it responds effectively instantaneously. Shoreline undulations on alongshore scales much smaller than the width of the shoreface will clearly not be reflected by contours extending to the base of the shoreface. In addition, changes in shoreline shape that occur on timescale shorter than the characteristic time for the whole shoreface to respond will not necessarily be reflected in the contours on the deeper portions of the shoreface. To address the evolution of shoreline features on these smaller time and space scales, wave transformation over contours that do not reflect the shoreline shapes of interest needs to be considered {Falqués, 2003 #1419;Falqués, 2005 #1433;Falqués, 2011 #1854}. For example, the smaller the alongshore scales of a coastline undulation, and the shallower the undulations affects the seabed (and the longer the wave period), the greater the dominance of high-angle waves at the offshore extent of the shoreface needs to be to cause the high-angle coastline instability {van den Berg, 2011 #1853;van den Berg, 2012 #1862}.

The simplified treatment of wave transformations in the work described here also neglects the alongshore redistribution of wave energy that curved bathymetric contours cause. Modeling of coastline morphodynamics that explicitly trace wave-ray paths shows that this concentration of energy near subtle shoreline promontories affects the rates of growth and migration of coastline features {Falqués, 2005 #1433;Falqués, 2011 #1854}. However, this effect become less important as the radius of coastline curvature becomes small relative to the width of the shoreface; again the simple wave-transformation treatment becomes most realistic at large alongshore scales.

The wave shadowing effect that a protruding portion of the coastline has is also simplified in this model (Figure 3). Although wave energy will be greatly reduced on a real coastline where other segments of the coastline block direct wave propagation, diffraction and refraction around the protruding coastline feature will cause some wave energy to leak into areas that would be considered completely in shadow in the model. This alongshore redistribution of wave energy produces a smoother alongshore variation in wave height (and alongshore sediment flux) than the abrupt end of a wave shadow in the model implies. However, because wave-approach directions in the model chang on a daily time scale—and with them the locations of the abrupt shadow terminations—over longer time scales, the effects of this unrealistic discontinuity do not accumulate in any location. Further work is underway to test the sensitivity of model behaviors to more realistic treatments of wave transformations when coastline shapes are complex.

Observations suggest that despite the simplified wave treatments, the model framework described here is relevant to natural coastline change. Utilizing multiple airborne (lidar) surveys of shoreline position along a nearly straight portion of the North Carolina Outer Banks (USA), analyses of patterns of coastline change show that the components of shoreline change with alongshore length scales of a few kilometers or greater exhibit a relationship between shoreline change and coastline curvature that is consistent with predictions of coastline diffusion {Lazarus, 2007 #1850;Lazarus, 2011 #1851;Lazarus, 2012 #1852}.

Analyses of local wave climates support model predictions regarding more complex coastline shapes. The emergent coastline shapes in the model always feature alongshore variations in the wave climates affecting coastline segments locally. These variations arise both from the changes in coastline orientation (changing the local frame of reference for approaching waves), and from wave shadowing effects (which filter out some of the high angle waves for more landward portions of the coastline). Where local wave climates have been analyzed for an extended portion of coastline, the trends of alongshore variance are consistent with those in the model {Ashton, 2006 #1469}.

Finally, comparisons between model results and the shapes of sandy coastlines (and the sandy shores of lakes and bays) in nature (e.g. Figure 7), and the relationship between those shapes and the wave climates {Ashton, 2001 #1788;Ashton, 2006 #1469;Thieler, 2011 #1864}, is consistent with the notion that the simple interactions in the model provide the basic explanation for a variety of coastline morphologies and behaviors.

References

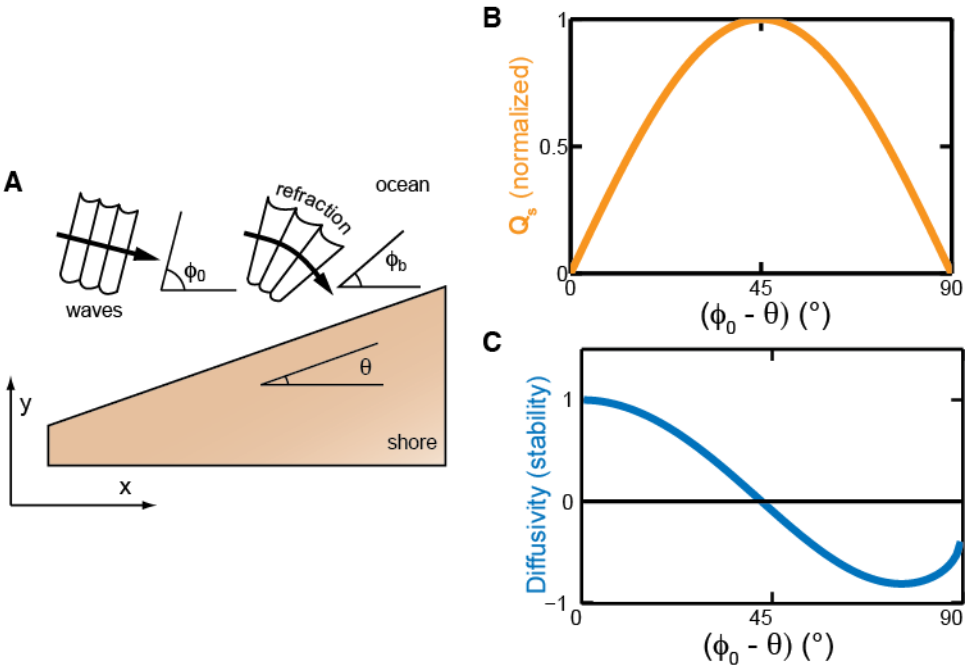

422

423

424 **Figure 1.** Key concepts of alongshore sediment transport and shoreline instability. A) Plan view showing
425 axes and reduction of wave angle due to refraction. B). Alongshore sediment transport as a function of
426 offshore wave angle. C.) Shoreline shape diffusivity as a function of deep-water wave angle.

427

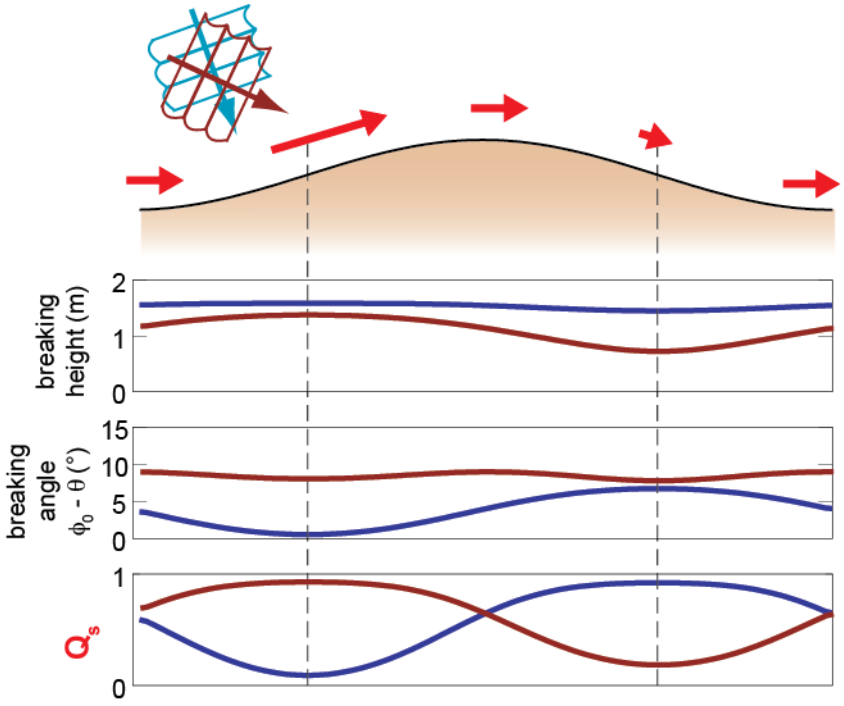

Figure 2. Computed wave values along a hypothetical shoreline undulation for both low-angle (20°, blue lines) and high-angle waves (65°, dashed lines). Vertical dashed lines indicate the location of the inflection points on the undulation. Values computed for wave height, *H*, 1m and wave period, *T*, 8s.

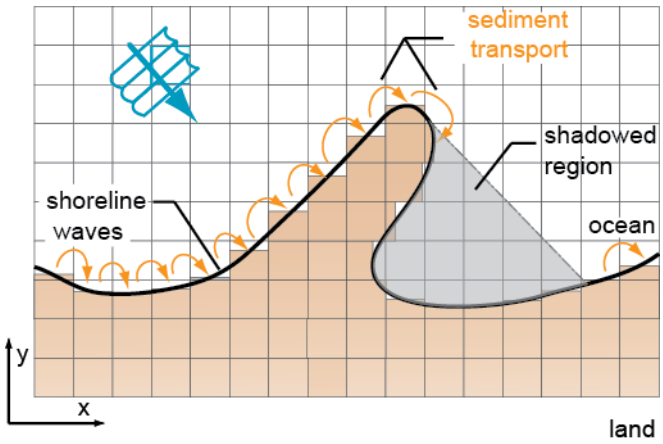

435

436

437 **Figure 3.** Model schematic demonstrating discretization of the plan view into discrete cells. For waves of
438 given orientation and height, sediment is transported along the shoreline using equation [2] and cell
439 quantities are adjusted based on flux gradients. Note also the zone 'shadowed' from wave approach;
440 sediment transport does not occur in shadowed regions.

441

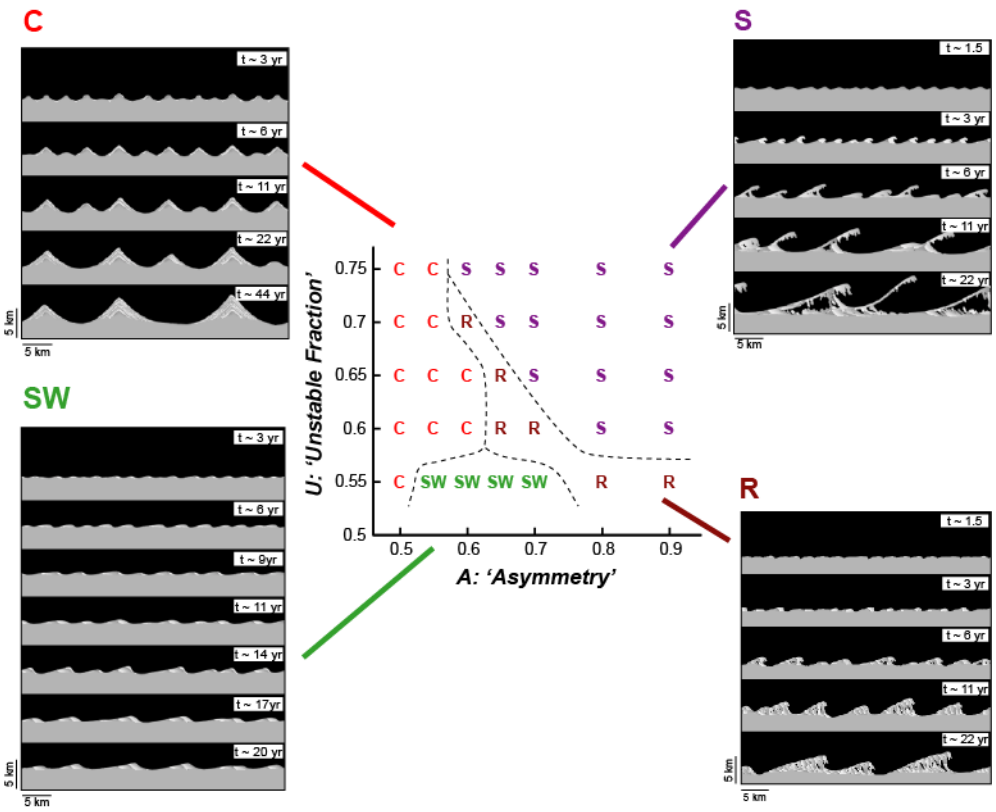

442

443 **Figure 4.** Model results for different angular distributions of approaching waves demonstrating how
444 wave attributes control the dominant morphological form of unstable coastline evolution.

445

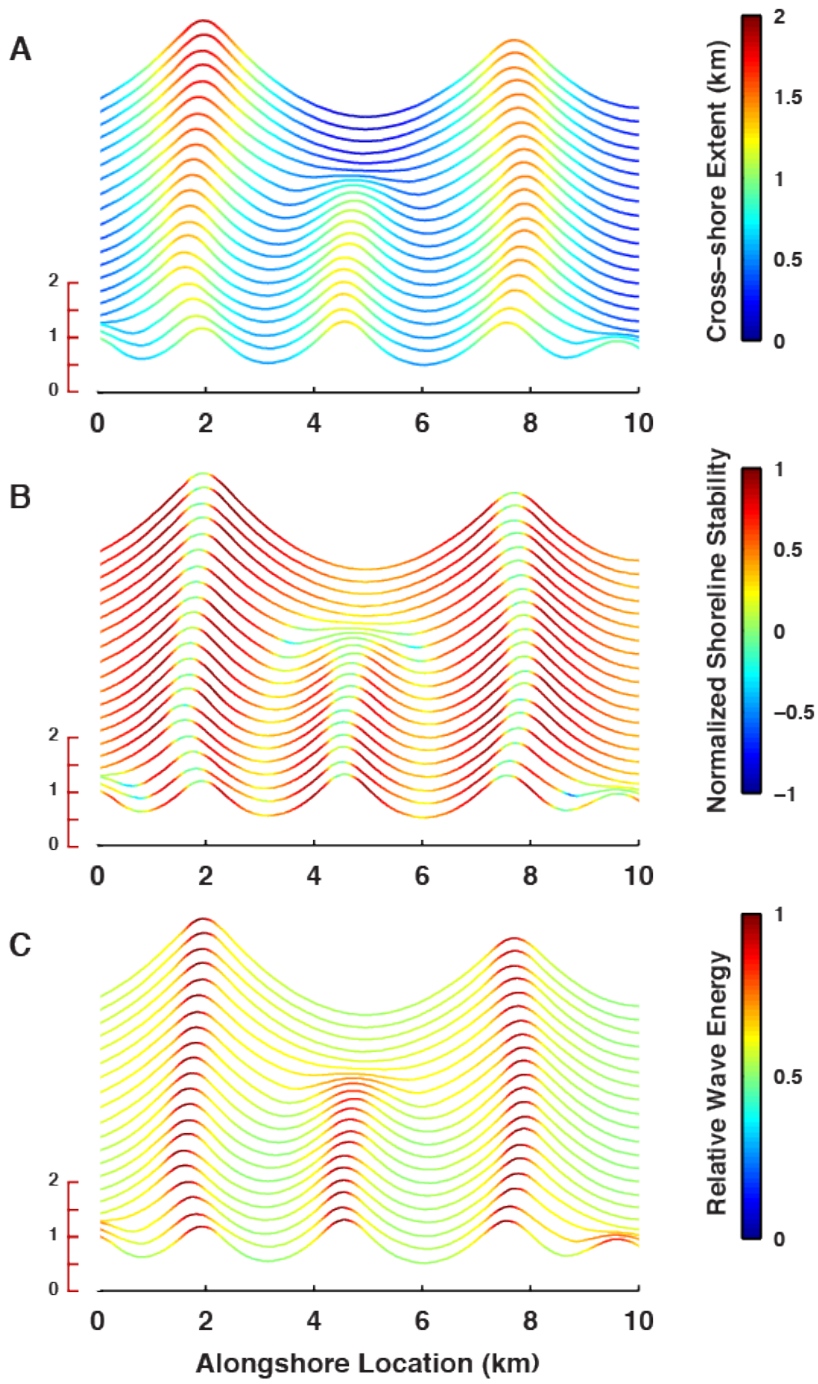

446

447 **Figure 5.** Timestacks of evenly spaced model shorelines (increasing time in the up direction) showing
448 cuspate cape coarsening with symmetric wave approach (A = 0.5, U = 0.7). Shorelines are colored by A)
449 cross-shore extent, B) local normalized shoreline diffusivity (or stability, with positive values stable and
450 negative values unstable), and C) relative wave energy (demonstrating the effects of shadowing by cape
451 tips).

452

453

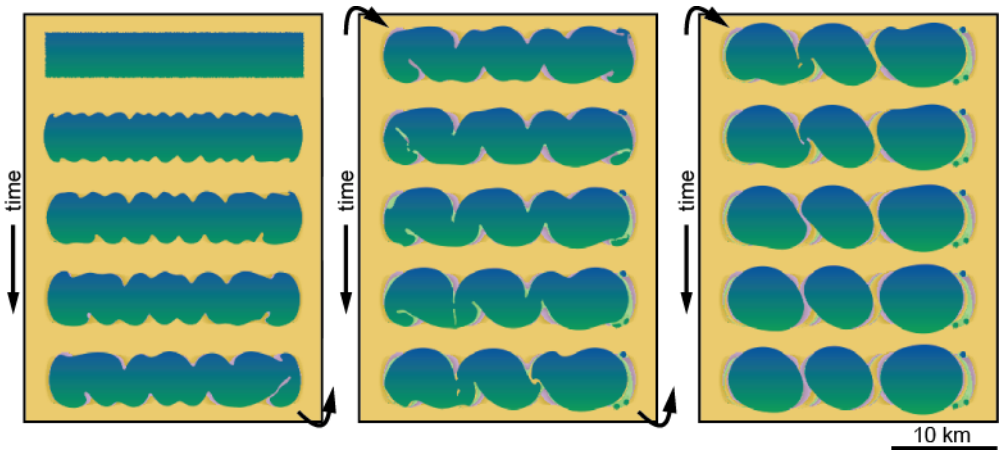

454

455

456 **Figure 6.** Modeled evolution of an elongate enclosed water with long-term symmetric distribution of
457 wind approach angle.

458

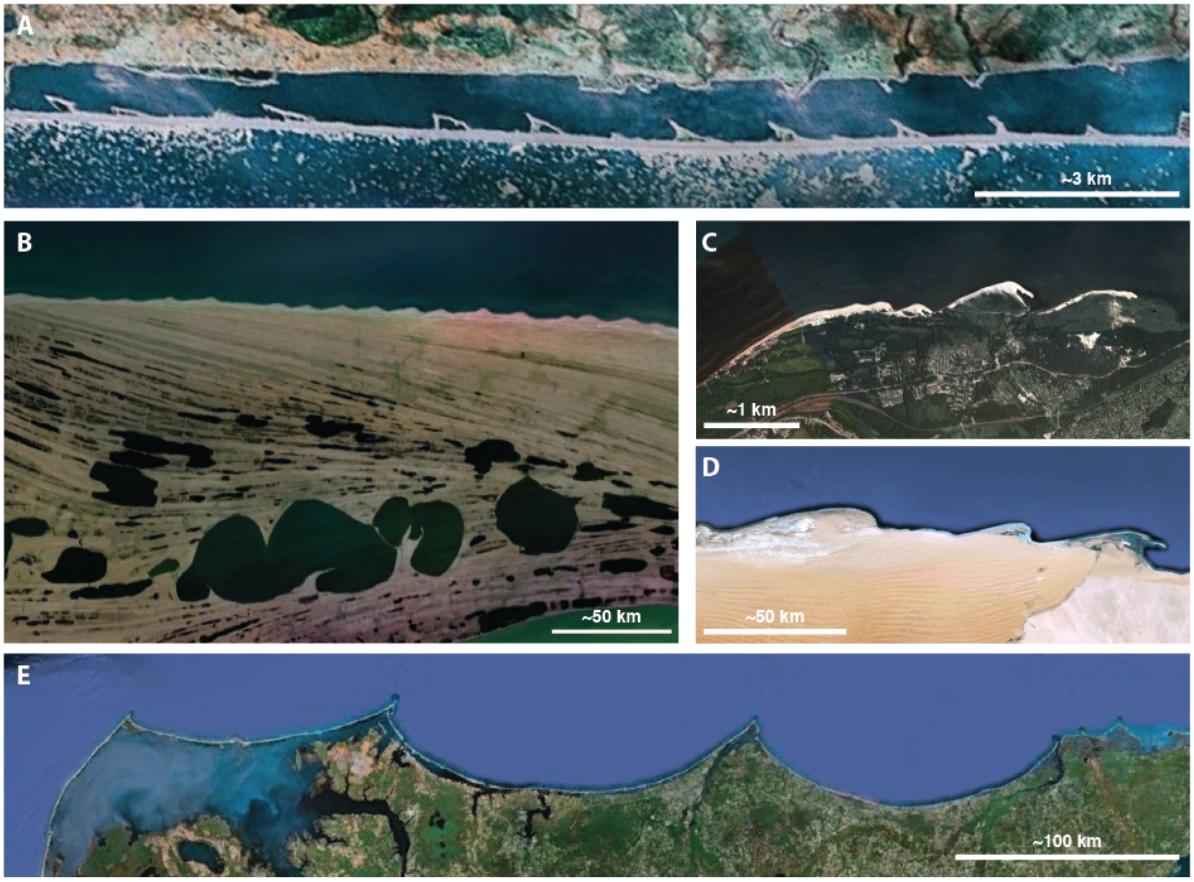

Figure 7. Natural examples of rhythmic shorelines. A) Russian Arctic coast, showing morphologies 'S' and 'R' from Figure 4, B) Cape Krusentern, Alaska, USA, showing on the open-ocean coast morphology 'SW' from Figure 4, and on the beach-ridge plain some of the enclosed water body phenomena in Figure 6, C) Russian coast near St. Petersburg, showing morphology 'R' in Figure 4, D) Namibian coast, showing morphology 'R' in Figure 4, E) Carolina coast, USA, showing morphology 'C' in Figure 4. Images copyright Google Earth.